*Acta Polytechnica CTU Proceedings* **44**:28–32, 2023
https://doi.org/10.14311/APP.2023.44.0028


# SIMULATION OF THE COMPRESSION TEST OF THE ZR1NB FUEL CLADDING RING

Vojtěch Smolík[a,*], Alžběta Endrychová[a,b], Jakub Krejčí[b]

[a] *Czech Technical University in Prague, Faculty of Mechanical Engineering, Department of Energy Engineering, Technická 4, 166 07 Praha 6, Czech Republic*

[b] *UJP PRAHA a.s., Nad Kamínkou 1345, 156 00 Praha-Zbraslav, Czech Republic*

[*] corresponding author: vojtech.smolik@fs.cvut.cz

Abstract. Fuel cladding is a first protective barrier against the loss of fission products that must withstand extreme conditions, from normal operation to final and interim dry storage. This hostile environment results in mechanical and microstructural damage of cladding caused by different stress levels, temperature, corrosion, hydrogen pick up and other degradation processes further enhanced by radiation. For this reason, the integrity of the cladding is a critical issue. The aim of this work is to simulate a ring compression test to evaluate the stress-strain behavior and hoop fracture properties of a zirconium-based alloy with niobium, which was chosen because it is widely used as fuel cladding in light water nuclear reactors.

Keywords: Zirconium, fuel cladding, ring compression test.

## 1. Introduction

Zirconium-based alloys have served the nuclear industry for more than 60 years due to their acceptable properties for the nuclear cores of light water reactors [1].

Zirconium-based cladding has low neutron absorption cross section and good mechanical and corrosion properties under normal operation in reactors [2].

The ZrlNb alloy designed in Russia has been in successful operation in the VVER and RBMK reactors since 1960. The Zr1Nb type cladding has been used in VVER reactors for many decades in different countries [1, 3].

Fuel cladding serves as the first barrier against the loss of fission products in the defense at depth during normal operation and subsequent storage. During operation, the cladding has to cope with different stress levels at high temperatures and neutron radiation. Understanding mechanical properties is very important.

Ring compression test is an important experimental technique used in materials science to evaluate the mechanical properties of various materials, including cladding alloys. In the nuclear industry, the mechanical behavior of the alloy cladding is critical to ensure safe and reliable operation of nuclear fuel rods.

A ring compression test was performed on the sample to determine the mechanical behavior of the Zr1Nb cladding alloy. The results of the test provide valuable insights into the deformation behavior of the Zr1Nb cladding alloy and its response to external forces.

The aim of this work is to compare the simulation results with the data from the conducted experiment.

| Name | T [°C] | l [mm] | h [mm] | t [mm] |
|---|---|---|---|---|
| T-RCT1 | 20 | 10,09 | 9,10 | 0,57 |
| T-RCT2 | 20 | 9,94 | 9,10 | 0,57 |
| T-RCT3 | 20 | 10,11 | 9,10 | 0,57 |
| T-RCT4 | 340 | 10,07 | 9,11 | 0,57 |
| T-RCT5 | 340 | 9,91 | 9,10 | 0,57 |
| T-RCT6 | 340 | 10,08 | 9,10 | 0,57 |

Table 1. Table containing the parameters of the samples: T is the temperature during the experiment, l is the length, h is the height, and t is the thickness.

## 2. Material and mechanical testing method

An INSTRON 1185 testing machine, equipped with a 100 kN load cell, was used to perform the ring compression test (RCT) for two sample temperatures (20 °C and 340 °C). The lengths of the ring samples, mechanically tested in this study, were $10.0 \pm 0.1$ mm. The length of tubular sample was chosen to have a plane strain state during compression test (length > outer diameter). Displacement-controlled tests were performed with a load line displacement rate of 0.5 mm/min. The load-displacement curves were continuously recorded.

RCT was performed on 6 unirradiated samples fabricated from the Zr1Nb alloy of the tubular section of UJP Prague. The chemical composition of the Zr1Nb coating tube was 99 % zirconium and 1 % niobium with minor impurities of Fe and O. The parametres of each sample are shown in Table 1. The picture of the T-RCT1 sample after RCT is shown in Figure 1.

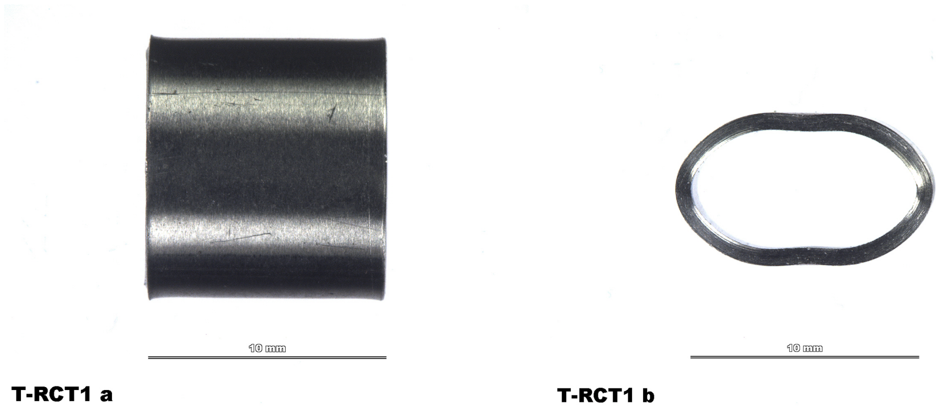


FIGURE 1. Sample after ring compression test.

| Name | $P_0$ [N] | UTS [MPa] |
|---|---|---|
| T-RCT1 | 372 | 378 |
| T-RCT2 | 366 | 380 |
| T-RCT3 | 377 | 380 |
| T-RCT4 | 159 | 162 |
| T-RCT5 | 158 | 164 |
| T-RCT6 | 154 | 157 |

TABLE 2. Table containing the collapse force and ultimate tensile strenght from RCT.

## 2.1. Determination of material properties

The collapse force $P_0$, where a large plastic deformation occurred, was obtained directly from the load-displacement curve by getting the intersection of the lines extended from the elastic and plastic regions [4]. After the collapse force is extracted from the load-displacement curve, the ultimate tensile stress (UTS) can be obtained. The collapse stress is calculated by equation [5, 6]

$$\sigma_0 = \frac{\alpha P_0 R}{t^2 L}, \tag{1}$$

where $\sigma_0$ is the collapse stress, the constant $\alpha$ depends on the length of the sample and for our case it is equal to 0.866, $P_0$ is the collapse force, $R$ is the radius of the sample, t is the thickness and L is the length.

The collapse stress is determined by the RCT and then it can be linearly correlated with the UTS of the tensile test through the following coefficients [4]

$$UTS = \frac{\sigma_0}{K_{UTS}}, \tag{2}$$

where $K_{UTS}$ is equal to 1.18.

The collapse force and the ultimate tensile strength for each sample are shown in Table 2.

Another important determined property of the material is Young's modulus, which indicates the ability of a material to resist longitudinal changes in tension or compression. Young's modulus is dependent on temperature, as can be seen in Figure 2 where a dependence is shown not only on temperature, but

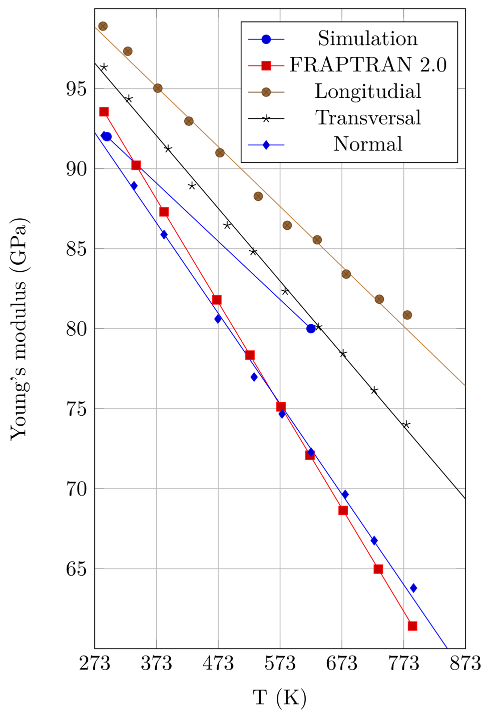


FIGURE 2. Comparison of different relations of Young's modulus of Zr1Nb on temperature: Results of the simulation (blue), values calculated using the Equation (3) of the FRAPTRAN 2.0 code (red), experimentally determined values by Rosigner et al. taken from [7] of Young's modulus in three main directions.

also on direction. Rosigner et al. [7] experimentally determined Young's elastic modulus at room temperature in the normal direction to be between 91.91 GPa and 92.96 GPa, in the longitudinal direction between 95.31 GPa and 96.42 GPa, and in the transversal direction between 95.5 GPa and 99.2 GPa. Young's elastic modulus for 350 °C (623 K) according to the graph is equal to 80 GPa for the normal direction, 73 GPa for the longitudinal direction, and 85 GPa for the transversal direction.

The equations for the determination of Young's modulus $E$ for a temperature lower than 1073 K were taken from [8, 9].

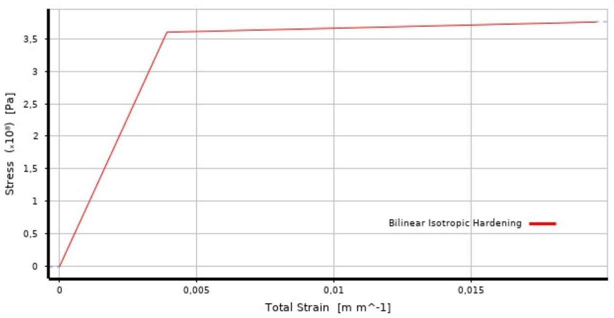


Figure 3. Stress-strain curve - Bilinear isotropic hardening model.

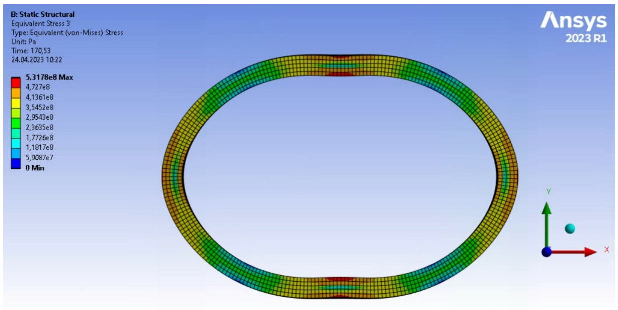


Figure 4. Numerical mesh with stress distribution in the sample.

$$E = 1.121 \cdot 10^{11} - 6.438 \cdot 10^{7} \cdot T[K]. \qquad (3)$$

This equation is used in FRAPTRAN 2.0 for Zr1Nb. Young's modulus for the uncoated zirconium alloy according to Equation (3) is E ≈ 93 GPa at room temperature and E ≈ 73 GPa at 340 °C. The values of Young's modulus were calculated by simulation and an attempt was made to match these values.

### 2.2. Numerical simulation

The simulation was done up to a deformation of 2 mm, because at this deformation it is already possible to observe whether the sample is sufficiently ductile or brittle. A numerical solution was performed in the static structural analysis ANSYS 2023 R1. The bilinear isotropic hardening model was applied to define the material properties of the tested sample. The example of bilinear isotropic hardening stress/strain material properties of the T-RCT1 sample is shown in Figure 3.

The displacement velocity of the test sample was set to match the experiment. Sensitivity analysis of the numerical mesh has also been performed. The mesh used is shown in Figure 4, it consists of 51 615 cells with a size setting of 0.15 mm.

The numerical solver has been set to a controlled time step, the duration of 2 mm displacement test is 240 s.

The numerical simulation will be used to further study the stress-strain distribution and hoop fracture behavior of new ATF fuel caldding concepts (accident tolerant fuel) with different mechanical properties and the comparison with the commonly used Zr1Nb alloy.

Severe accidents in LWRs led to research of new materials used as fuel cladding to improve nuclear safety during normal and possible accident conditions. Protective coatings deposited on Zr alloys as substrates are one of the most perspective near-term concepts of ATF.

Thin layers of Cr, CrN or multilayers such as CrNCr are deposited on the Zr alloy substrate by various methods. These protective coatings are used to improve the mechanical and corrosion properties of typically used Zr alloys under accident conditions.

The future work will be focused on the numerical simulations and determination of the material properties of Zr1Nb with Cr, CrN and CrNCr coating, which are shown in Figure 5. The Zr alloy coating can make a significant change in the mechanical properties of the samples. For example, Young's modulus of chromium at room temperature is E ≈ 290 GPa [10]. The modulus of elasticity of an uncoated Zr1Nb sample is approximately three times smaller than the modulus of elasticity of the chromium sample. For these reasons, studying the effect of the coating on the overall mechanical behavior of the cladding and the failure mode of the coating (ductile or brittle) is important for the mechanical integrity of the Cr coating as the most encouraging candidate among different types of coatings.

Another approach is to study the influence of the hydrogen content on the stress-induced precipitation of radial hydride in the fuel cladding. Hydrogen pickup is caused by the oxidation of the fuel rod. The hydrogen produced by this reaction is absorbed by cladding and can be dissolved in the crystal lattice or precipitated to create hydrides. Hydrogen removal degrades the mechanical properties of the cladding and can cause fuel rod failure. Radial hydride embrittement was considered a key phenomenon to be taken into account in dry storage studies [11].

## 3. Results and discussion

Figure 6 shows a comparison of the numerical and experimental results of the fuel cladding samples at two different temperatures. It can be seen that the numerical results perform a force reaction lower than the experimental values for both test samples.

The reaction force of the tested sample is plotted in relation to the displacement of the sample.

The contours of the von Mises stress of the tested sample are shown in Figure 7. The stress distribution in the numerical simulation is in agreement with the observed crack mechanics of the fuel cladding samples for larger displacements. 1 mm and 2 mm displacements are presented, and the maximum stress is observable in the areas near the contact between the test sample and the compression test device. The stress distribution from the numerical results can also

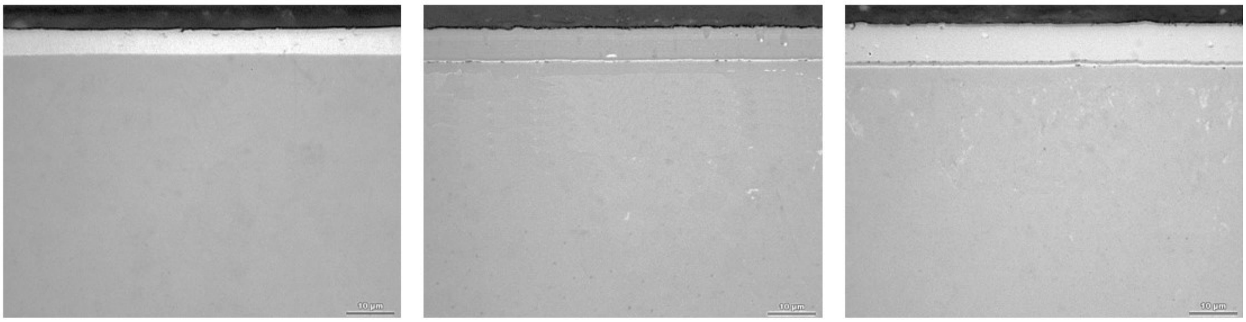

FIGURE 5. Zr1Nb alloy with different coatings deposited by PVD method – Cr, CrN and multilayer CrNCr.

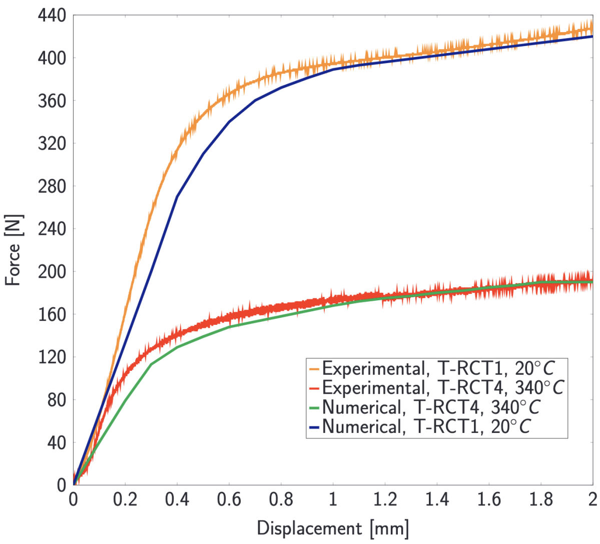


FIGURE 6. Force-displacement curves – Experimental and numerical results.

correctly determine the areas of tensile and compressive stress, an important factor for the calculation of the UTS (ultimate tensile strength) and YS (yield strength) from the RCT.

The hoop fracture mechanics is not included in the numerical simulation at this stage of the research, so only displacements up to 2 mm are considered. The Young's modulus value was determined from the simulation to be 92 GPa at room temperature and 80 GPa at 340 °C. The values are plotted in Figure 2, compared to the experimentally measured values and the correlation used in FRAPTRAN 2.0. The figure also shows that the value determined by the simulation for room temperature is appropriate. For higher temperatures, the value of the Young's modulus is higher than the prediction of FRAPTRAN 2.0. This could be due to a slightly different chemical composition of the sample material. Although it is also a Zr1Nb alloy with 1 wt. % niobium, the contribution of impurities such as Fe, O, or Hf was diverse. The FRAPTRAN 2.0 code is based on the equations of Vokovo et al. [9] from 1989, and a study on the Young's modulus by Rosigner et al. [7] was published in 1978. The alloy composition has changed over the years and with the development of the nuclear power industry. For example, the process of removing hafnium from zirconium, which has a neutron absorption cross section 600 times higher than that of zirconium, improved, and the oxygen and iron content also changed, significantly influencing the mechanical properties. Currently, the Zr1Nb alloy, commercially named E110, contains 500-700 ppm of O and 100 ppm of Fe [12]. The Zr1Nb alloy used by Rosigner et al. [7] in 1978 contained 800 ppm O and no Fe.

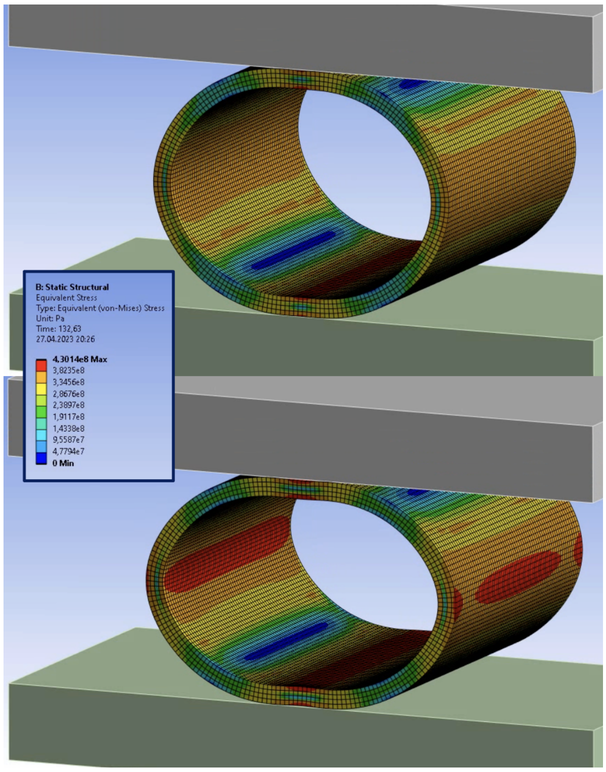


FIGURE 7. von-Mises stress contour result of numerical simulation, T-RCT1 sample, 1 mm displacement (up) and 2 mm displacement (down).

## 4. CONCLUSION

Ring compression test is an important and simple method that is used to determine mechanical properties in the hoop direction, which is essential for the integration of fuel cladding.

Numerical and experimental results of the ring compression test are presented. The yield stength for 20 °C and 340 °C was determined using the iterative method. The resulting load-displacement curves of numerical and experimental work are compared.

The collapse load and the ultimate tensile strength were determined from the load-displacement curves. Young's modulus of elasticity was determined and compared with the values found in the literature.

Numerical simulation represents a new approach to evaluate the von Mises stress distribution in the test sample and predict the areas with the highest stress load.

Numerical model developed in this study will be extended to include the mechanics of crack formation.

## Acknowledgements

The authors wish to thank the entire Zirconium Alloys Team at UJP PRAHA a.s.

## References

[1] R. Comstock, P. Barbéris. *Zirconium in the Nuclear Industry: 17th International Symposium.* Journal of ASTM International: Selected technical papers. ASTM International, 2015. ISBN 9780803175297.

[2] E. Perez-Feró, C. Győri, L. Matus, et al. Experimental database of E110 claddings exposed to accident conditions. *Journal of Nuclear Materials* **397**(1):48–54, 2010. `https://doi.org/10.1016/j.jnucmat.2009.12.005`

[3] *Design and Performance of WWER Fuel.* No. 379 in Technical Reports Series. International Atomic Energy Agency, Vienna, 1996.

[4] H. Namburi, L. Ottazzi, M. Chocholousek, et al. Study hydrogen embrittlement and determination of E110 fuel cladding mechanical properties by ring compression testing. *IOP Conference Series: Materials Science and Engineering* **461**(1):012059, 2018. `https://doi.org/10.1088/1757-899X/461/1/012059`

[5] V. Busser, J. Desquines, C. Duriez, et al. Zircaloy-4 cladding hydride reorientation under ring compression test conditions. In *Proceedings of Top Fuel 2009.* 2009. `https://doi.org/10.13140/2.1.2563.9363`

[6] T. Yella Reddy, S. Reid. On obtaining material properties from the ring compression test. *Nuclear Engineering and Design* **52**(2):257–263, 1979. `https://doi.org/10.1016/0029-5493(79)90055-4`

[7] H. Rosinger, D. Northwood. The elastic properties of zirconium alloy fuel cladding and pressure tubing materials. *Journal of Nuclear Materials* **79**(1):170–179, 1979. `https://doi.org/10.1016/0022-3115(79)90444-6`

[8] W. G. Luscher, K. J. Geelhood. Material property correlations: Comparisons between FRAPCON-3.4, FRAPTRAN 1.4, and MATPRO. Tech. rep., Pacific Northwest National Lab. (PNNL), Richland, WA (United States), 2010. `https://doi.org/10.2172/1030897`

[9] W. G. Luscher, K. J. Geelhood. Material property correlations: Comparisons between FRAPCON-3.5, FRAPTRAN-1.5, and MATPRO, 2014. U.S.NRC: NUREG/CR-7024, Rev. 1, PNNL-19417, Rev. 1, [2023-11-17]. `https://www.nrc.gov/docs/ML1429/ML14296A063.pdf`

[10] D. V. Nguyen, M. Le Saux, L. Gélébart, et al. Mechanical behavior of a chromium coating on a zirconium alloy substrate at room temperature. *Journal of Nuclear Materials* **558**:153332, 2022. `https://doi.org/10.1016/j.jnucmat.2021.153332`

[11] J. Desquines, D. Drouan, M. Billone, et al. Influence of temperature and hydrogen content on stress-induced radial hydride precipitation in zircaloy-4 cladding. *Journal of Nuclear Materials* **453**(1):131–150, 2014. `https://doi.org/10.1016/j.jnucmat.2014.06.049`

[12] F. Onimus, S. Doriot, J.-L. Béchade. 3.01 – radiation effects in zirconium alloys. In R. J. Konings, R. E. Stoller (eds.), *Comprehensive Nuclear Materials (Second Edition)*, pp. 1–56. Elsevier, Oxford, second edition edn., 2020. `https://doi.org/10.1016/B978-0-12-803581-8.11759-X`